Journal of Materials Chemistry A

Superior electrochemical performance of Li3VO4/N-doped C as anode for Li-ion batteries

Journal:	*Journal of Materials Chemistry A*
Manuscript ID:	TA-COM-06-2015-004402.R1
Article Type:	Communication
Date Submitted by the Author:	30-Jul-2015
Complete List of Authors:	Ni, Shibing; three gorges university, College of Mechanical and Material Engineering Zhang, Jicheng; Three Gorges university, material and chemical engineering Ma, Jianjun; Three Gorges university, material and chemical engineering Yang, Xuelin; Three Gorges university, material and chemical engineering Zhang, Lulu; Three Gorges university, material and chemical engineering

Cite this: DOI: 10.1039/c0xx00000x

www.rsc.org/xxxxxx

ARTICLE TYPE

Superior electrochemical performance of Li_3VO_4/N-doped C as anode for Li-ion batteries

Shibing Ni,*[a,b] Jicheng Zhang,[a] Jianjun Ma,[a] Xuelin Yang,*[a,b] and Lulu Zhang[a,b]

Received (in XXX, XXX) Xth XXXXXXXXX 201X, Accepted Xth XXXXXXXXX 201X

DOI: 10.1039/b000000x

High performance Li_3VO_4/N-doped C anode was successfully prepared, which delivers initial discharge/charge capacity of 600/472 mAh g^{-1} at 150 mA g^{-1}, maintaining of 462/460 mAh g^{-1} after 100 cycles. It shows no capacity attenuation over 2200 cycles at 2000 mA g^{-1}, delivering discharge/charge capacity of 267/264 mAh g^{-1}.

Lithium vanadate, Li_3VO_4 shows safer discharge plateau than graphite and lower voltage plateau and higher capacity than $Li_4Ti_5O_{12}$,[1] which is demonstrated to be a promising anode for Li-ion batteries. However, the electronic conductivity of Li_3VO_4 is low compared to its ionic conductivity,[1,2] which may cause a large polarization in charge/discharge process. As results, on the one hand, the lithiation degree of Li_3VO_4 attenuates distinctly along with the increasing of particle size. On the other hand, the specific capacity of Li_3VO_4 decreases sharply along with the increasing of specific current, showing unsatisfied rate performance. Previous research has demonstrated that improving the electronic conductivity of Li_3VO_4 can distinctly enhance its electrochemical performance. Attempts on combining Li_3VO_4 with carbonaceous materials such as graphene, carbon nanotubes, amorphous carbon and natural graphite as well as depositing Li_3VO_4 on Ni foam have been tried to improve the electrochemical performance of Li_3VO_4, which have gained impressive results.[2-7]

Recently, it has been reported that N-doped carbon (N-C) supported materials can further improve the cycle performance and rate capability owing to the improved electronic conductivity, ion permeability of the carbon layer, charge transfer at the interface and stability of the SEI films. For example, N-C coated Fe_3O_4 delivers capacity retention of 99% after 100 cycles at 500 mA g^{-1} and subsequent 100 cycles at 1000 mA g^{-1}.[8] MnO/N-C exhibits specific capacity of 982 mAh g^{-1} after 100 cycles at 500 mA g^{-1}.[9] $Li_4Ti_5O_{12}$ coated with N-C shows 124 mAh g^{-1} after 2200 cycles at 2C.[10] It is thus reasonable to believe that combining Li_3VO_4 with N-C can further improve its electrochemical performance. However, research on Li_3VO_4/N-C has not been reported by now.

In our previous study, we fabricated Li_3VO_4 via a solution based method.[11] It was found that the intermedial solution phase can improve the homogeneity of the final products, which will be beneficial for symmetrical N-C combination at nanoscale. Here in this paper, we report the preparation of Li_3VO_4/N-C via introducing hexamethylenetetramine in the intermedial solution, which can act as both carbon source and N-doping agent.[12] In the subsequent sintering process, the generation of Li_3VO_4 and the formation of N-C occur simultaneously, resulting in the formation of Li_3VO_4/N-C composite architecture. On the one hand, the N-C layer can distinctly improve the electronic conductivity of the composite, and the N-C layer can prevent the growth of Li_3VO_4 particles, maintaining high electrochemical activity. On the other hand, good contact between Li_3VO_4 and N-C layer can improve the structure stability of the Li_3VO_4/N-C electrode in cycling. As results, the as-prepared Li_3VO_4/N-C shows superior electrochemical performance as anode for Li-ion batteries.

Typical XRD pattern of the products is shown in Fig. 1(a). As seen, the diffraction peaks located at 16.3°, 21.5°, 22.8°, 24.3°, 28.1°, 32.8°, 36.3°, 37.7°, 49.7°, 58.6°, 66.2° and 70.9° can be attributed to the (100), (110), (011), (101), (111), (200), (002), (201), (202), (320), (203) and (322) faces of orthorhombic Li_3VO_4 with lattice constants a=6.319 Å, b=5.448 Å and c=4.940 Å, which is in good agreement with JCPDS, no. 38-1247. Fig. 1(b) is the Raman spectrum of the products. Apart from typical Raman peaks of Li_3VO_4, two strong peaks near 1356 and 1582 cm^{-1} can ascribe to disorder phase (D-band) and graphite phase (G-band) of carbon.[6,13] The results indicate Li_3VO_4/C composite is successfully prepared. Furthermore, the composition of the Li_3VO_4/C was further characterized by XPS. As shown in Fig. 1(c), the survey spectrum confirms the presence of O, V, N and C in the products. The high resolution spectrum of V2p is shown in Fig. 1(d), which can be divided into four peaks. The peaks at 524.7 and 517.1 eV can ascribe to $V2p_{1/2}$ and $V2p_{3/2}$ of V^{5+} spin-orbit levels, whereas the peaks at 521.7 and 516.2 eV can be attributed to $V2p_{1/2}$ and $V2p_{3/2}$ of V^{4+} spin-orbit levels.[14] Fig. 1(e) is the high resolution spectrum of C1s, which can be fitted by three peaks. The peak at 284.4 eV corresponds to the C-C bond in graphite-like sp^2 C,[15-17] the peak near 285.6 can ascribe to C-N or C≡N,[10,18] and the peak near 289.6 eV can be attributed to O-C=O chemical bonds.[18-20] The high resolution spectrum of N1s is shown in Fig. 1(f), which can be divided into three peaks. The peaks near 398.1 and 400.3 eV correspond to pyridinic and

pyrrolic N, respectively, and the peak near 399.1 eV can ascribe to C-N or C≡N.[9,15,18] According to the XRD, Raman and XPS results, it can be confirmed that Li_3VO_4/N-C composite architecture is successfully prepared.

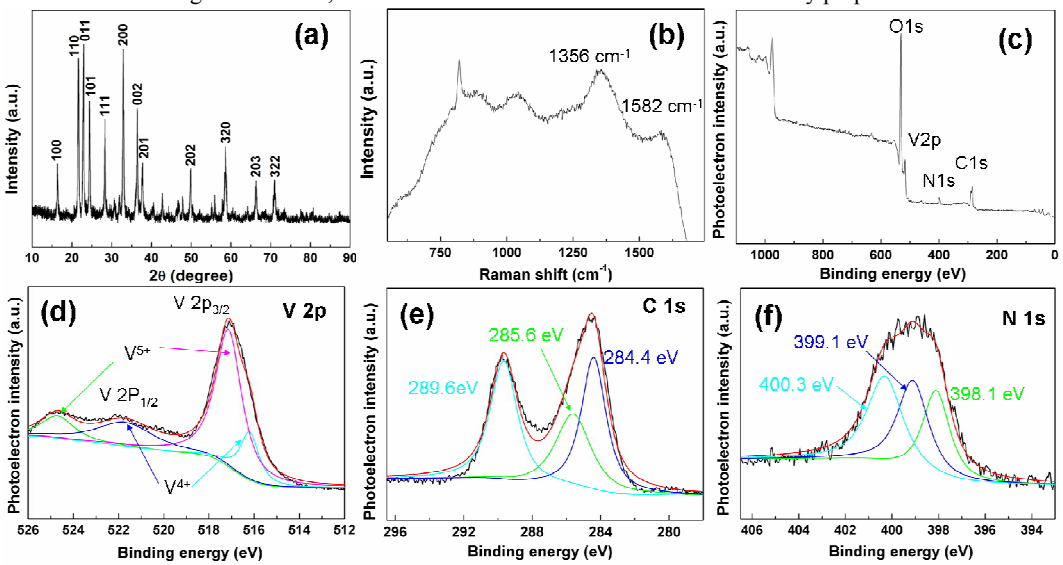

Fig. 1 (a) XRD pattern, (b) Raman spectrum and (c)-(f) XPS spectra of the Li_3VO_4/N-C. (c) The survey spectrum; High resolution spectrum of (d) V2p, (e) C1s and (f) N1s.

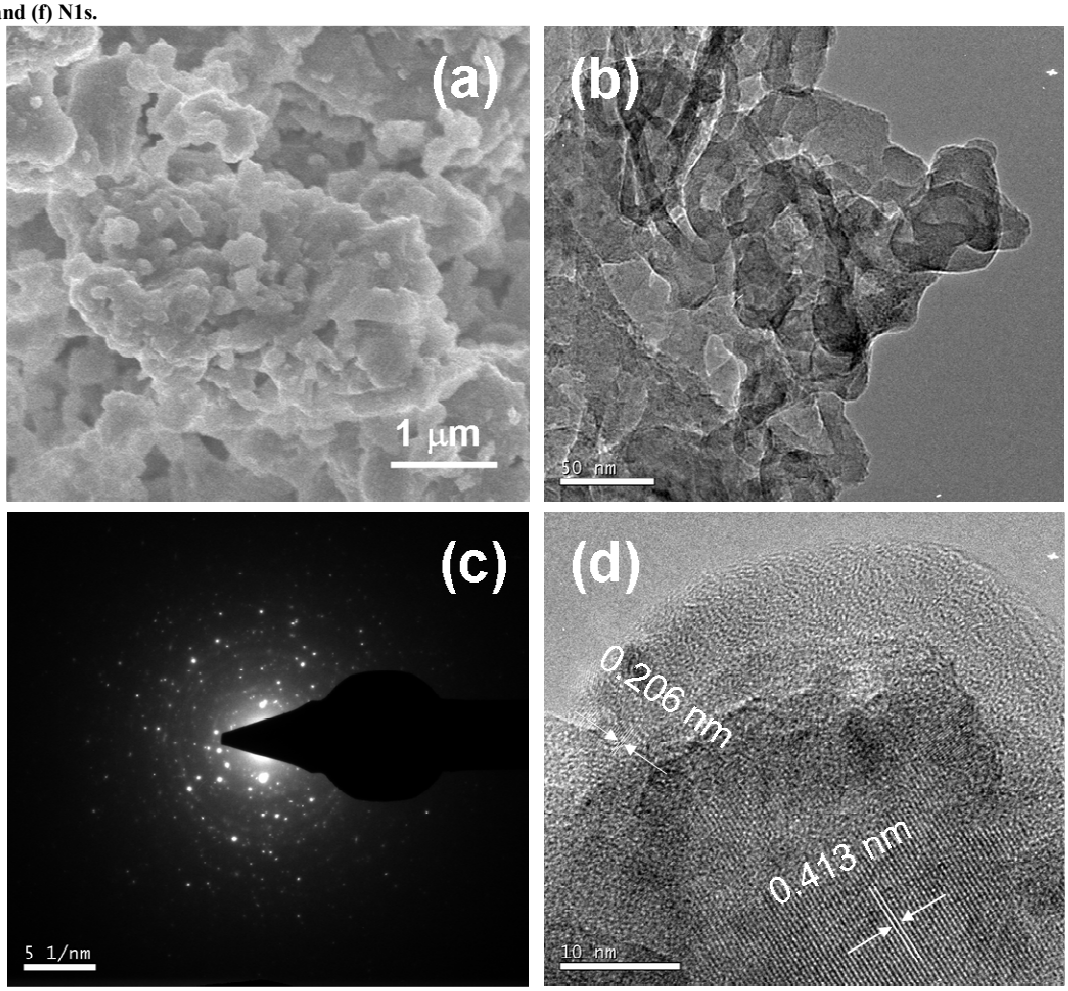

Fig. 2 (a) SEM, (b) TEM image, (c) SAED pattern and (d) HRTEM image of the Li_3VO_4/N-C.

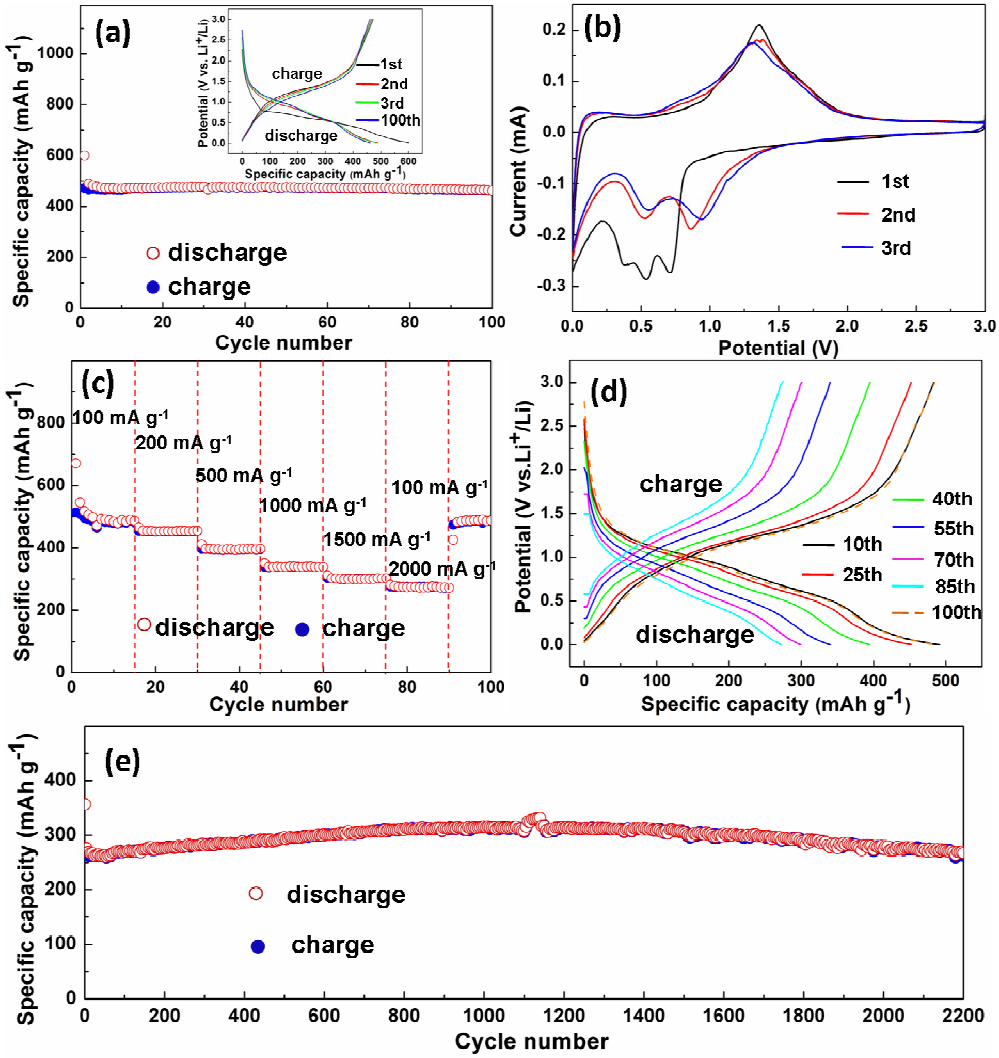

Fig. 3 Electrochemical performance of the Li_3VO_4/N-C electrode. (a) Capacity retention at a specific current of 150 mA g^{-1}. The inset of (a) is the charge/discharge curves for the initial three and the 100th cycles. (b) The initial three cyclic voltammograms at a scan rate of 0.2 mV s^{-1}. (c) Capacity retention and (d) representative charge and discharge curves of the Li_3VO_4/N-C electrode at various specific currents. (e) Long cycle performance of the Li_3VO_4/N-C electrode at a specific current of 2000 mA g^{-1}.

Fig. 2(a) is a low magnification SEM image of the as-prepared products, which exhibits a large number of nanoparticles with mean size about 300 nm. Meanwhile, EDS elemental mapping demonstrates clearly the presence of V, O, C and N element in the products (see ESI, Fig. s1), suggesting the successful preparation of Li_3VO_4/N-C. For further studying the microstructure of the Li_3VO_4/N-C, a TEM image is characterized and shown in Fig. 2(b). As seen, these nanoparticles are composed of a large number of small particles with mean size about 40 nm. Fig. 2(c) is a SAED pattern of the Li_3VO_4/N-C, which exhibits irregular diffraction spots, suggesting the polycrystalline characteristics of Li_3VO_4. Meanwhile, weak diffraction rings can be attributed to amorphous C. The microstructure of the Li_3VO_4/N-C was also testified by HRTEM image. As shown in Fig. 2(d), the interplanar spacing for the nanoparticle is 0.413 and 0.206 nm, which corresponds to the (110) and (220) face of orthorhombic Li_3VO_4, respectively. The amorphous layer with a thickness about 8 nm can ascribe to C in the Li_3VO_4/N-C.

Galvanostatic charge/discharge cycling was carried out in the potential window of 0.02~3.0 V versus Li. Fig. 3(a) shows the capacity retention and the initial three and 100th charge/discharge voltage profiles of the Li_3VO_4/N-C electrode at a specific current of 150 mA g^{-1}. As seen, the initial discharge curve differs slightly from the subsequent ones, showing two sloping potential regions (1.5~0.8 and 0.8~0.02 V), which correspond to the insertion of lithium ions into Li_3VO_4/N-C and the formation of solid electrolyte interface (SEI).[1,3,6,7,11] The subsequent discharge curves show similar profiles with two sloping potential regions (1.5~0.4 and 0.4~0.02 V), accompanied by capacity attenuation. All the charge curves exhibit similar profile with a sloping potential region from 0.8 to 2.5 V, corresponding to the extraction of lithium ions from Li_3VO_4.[3,6,7,11] The initial discharge capacity is 600 mAh g^{-1}, which is bigger than the charge capacity (472 mAh g^{-1}) owing to the formation of SEI.[1,11] Remarkably, the Li_3VO_4/N-C shows superior cycle performance, which delivers discharge and charge capacities of 462 and 460 mAh g^{-1} after 100 cycles. The electrochemical performance of the Li_3VO_4/N-C shows distinct improvement compared with those reported in

literature (capacity comparison see ESI, tab. s1†).[1-3,11,21-24] The high specific capacity of the Li_3VO_4/N-C is relevant to its specific architecture. In the Li_3VO_4/N-C, the small size of Li_3VO_4 is a guarantee of short diffusion pathway of lithium ions, and the N-C layer can provide high electron transfer efficiency (EIS spectra and the fitted electrochemical kinetic parameters of pristine Li_3VO_4 and the Li_3VO_4/N-C see ESI, Fig. s2 and tab. s2), which result in enhanced electrochemical reaction kinetics, improving the lithiation degree of the Li_3VO_4/N-C. Meanwhile, the good contact between Li_3VO_4 and N-C layer can provide stable charge transfer process in cycling (EIS spectra and the fitted electrochemical kinetic parameters of the Li_3VO_4/N-C in cycling see ESI, Fig. s3 and tab. s3), resulting in excellent cycle stability.[25] The effect of N-C on the electrochemical performance of Li_3VO_4/N-C electrodes was also evaluated. The presence of N-C can improve the specific capacity of the electrode,[26] and an appropriate amount of hexamethylenetetramine is beneficial to obtain the highest specific capacity (cycle performance of pristine and Li_3VO_4/N-C obtained with different amount of hexamethylenetetramine see ESI, Fig. s4). The cyclic voltammetric (CV) curves of the Li_3VO_4/N-C electrode were tested over a voltage region from 0 to 3.0 V at a scan rate of 0.2 mV s^{-1}. As shown in Fig. 3(b), the profiles of CV curves for the 2nd and 3rd cycle are similar, whereas an obvious difference between the first and the subsequent two cycles is found. In the 1st cathodic scan, three obvious reduction peaks at around 0.71, 0.52 and 0.35 V are observed, which correspond to the insertion of lithium ions into Li_3VO_4 and the formation of SEI.[3,6,7,11] Remarkably, the reduction peak near 0.35 V was not observed for most Li_3VO_4, whereas a weak reduction peak of Li_3VO_4/C near 0.35 V accompanies by distinct improvement of capacity.[3,7,11,23] Thus it can be deduced that the observation of clear reduction peak near 0.35 V is relevant to the enhanced lithiation of the Li_3VO_4/N-C. The reduction peaks shift to 0.48 and 0.76 V in the 2nd cathodic scan and 0.54 and 0.84 V in the 3rd cycle, which can ascribe to the activation of the Li_3VO_4/N-C electrode, being similar to that reported in literature.[3,6,7,11] The profiles for the initial three anodic scan are similar, showing an oxidation peak near 1.37 V, which is attributed to the delithiation process that can be described as: $Li_{3+x}VO_4 \rightarrow xLi^+ + Li_3VO_4 + xe^-$ ($x \leq 3$).[3,6,11,21,22] Fig. 3(c) shows the discharge and charge curves of the Li_3VO_4/N-C electrode at various specific currents from 100 to 2000 mA g^{-1}. Along with the increasing of specific currents, the discharge and charge capacities decrease owing to the enhanced polarization.[1,2,11] The 10th discharge capacity is 485, 454, 396, 339, 301 and 274 mAh g^{-1} at specific currents of 100, 200, 500, 1000, 1500 and 2000 mA g^{-1}, respectively. After that, the 10th discharge capacity can restore to 488 mAh g^{-1} when reverting the specific current to 100 mA g^{-1}, suggesting good recover ability. The rate performance of the Li_3VO_4/N-C shows distinct improvement compared with that of pristine Li_3VO_4 (see ESI, Fig. s5). Representative discharge and charge curves are shown in Fig. 3(d). As seen, the discharge potential decreases and the charge potential increases along with the increasing of specific current owing to polarization. However, when reverting the specific current to 100 mA g^{-1}, the representative charge and discharge curves show almost the same profiles to those of the 10th cycle, demonstrating highly stable electrochemical reactions in cycling.

The Li_3VO_4/N-C electrode also exhibits predominant long life performance. As shown in Fig. 3(e), the Li_3VO_4/N-C electrode shows discharge and charge capacities of 357 and 264 mAh g^{-1} in the initial cycle at a specific current of 2000 mA g^{-1}, which maintain of 267 and 264 mAh g^{-1} after 2200 cycles, showing no capacity attenuation in cycling. The superior electrochemical performance, the facile fabrication method, and the low cost endow the Li_3VO_4/N-C with practical application in Li-ion batteries.

In summary, Li_3VO_4/N-doped C was successfully prepared via a facile way, which shows superior electrochemical performance as anode for Li-ion batteries owing to the enhanced lithiation degree, electronic conductivity and structure stability. The reversible capacity of the Li_3VO_4/N-C can research 460 mAh g^{-1} after 100 cycles at a specific current of 150 mA g^{-1}, and 264 mAh g^{-1} after 2200 cycles at a specific current of 2000 mA g^{-1}. Meanwhile, the facile fabrication method reported here is facile and low cost, which is beneficial for the practical application of the Li_3VO_4/N-C in Li-ion batteries.

Acknowledgement

We gratefully acknowledge the financial support from Natural Science Foundation of China (NSFC, 51302152, 51272128, and 51302153). Moreover, the authors are grateful to Dr. Jianlin Li at Three Gorges University for his kind support to our research.

Notes and references

[a] *College of Materials and Chemical Engineering, China Three Gorges University, 8 Daxue Road, Yichang, Hubei 443002, China*
[b] *Hubei Provincial Collaborative Innovation Center for New Energy Microgrid, China Three Gorges University +86 717 6397505. E-mail address: shibingni07@126.com. xlyang@ctgu.edu.cn*

† Electronic Supplementary Information (ESI) available: [details of any supplementary information available should be included here]. See DOI: 10.1039/b000000x/

1 H.Q. Li, X.Z. Liu, T.Y. Zhai, D. Li and H.S. Zhou, Adv. Energy Mater., 2012, **3,** 428-432.
2 Z. Shi, J.Z. Wang, S.L. Chou, D. Wexler, H.J. Li, K. Ozawa, H.K. Liu and Y.P. Wu, Nano Lett., 2013, **13,** 4715-4720.
3 Z.Y. Liang, Y.M. Zhao, L.Z. Ouyang, Y.Z. Dong, Q. Kuang, X.H. Lin, X.D. Liu and D.L. Yan, J. Power Sources, 2014, **252,** 244-247.
4 Q.D. Li, J.Z. Sheng, Q.L. Wei, Q.Y. An, X.J. Wei, P.F. Zhang and L.Q. Mai, Nanoscale, 2014, **6,** 11072-11077.
5 J. Liu, P.J. Lu, S.Q. Liang, J. Liu, W.J. Wang, M. Lei, S.S. Tang and Q. Yang, Nano Energ., 2015, **12**, 709-724.
6 Z.L. Jian, M.B. Zheng, Y.L. Liang, X.X. Zhang, S. Gheytani, Y.C. Lan, Y. Shi and Y. Yao, Chem. Comm., 2015, **51**, 229-231.
7 S.B. Ni, X.H. Lv, J.C. Zhang, J.J. Ma, X.L. Yang and L.L. Zhang, Electrochim. Acta, 2014, **145,** 327-334.
8 C. Lei, F. Han, D. Li, W.C. Li, Q. Sun, X.Q. Zhang and A.H. Lu, J. Mater. Chem. A, 2015, **3**, 1168-1175.
9 X. Gu, J. Yue, L. Chen, S. Liu, H.Y. Xu, J. Yang, Y.T. Qian and X.B. Zhao, J. Mater. Chem. A, 2015, **3**, 1037-1041.
10 L. Zhao, Y.S. Hu, H. Li, Z.X. Wang and L.Q. Chen, Adv. Mater., 2011, **23**, 1385-1388.
11 S.B. Ni, X.H. Lv, J.J. Ma, X.L. Yang and L.L. Zhang, J. Power Sources, 2014, **248,** 122-129.
12 J.H. Kim, D. Bhattacharjya and J.S. Yu, J. Mater. Chem. A, 2014, **2**, 11472-11479.
13 Y.C. Du, X.S. Zhu, L. Si, Y.F. Li, X.S. Zhou and J.C. Bao, J. Phys. Chem. C 2015, 119, 15874-15881.
14 G. Silversmit, D. Depla, H. Poelman, G.B. Marin and R.D. Gryse, J. Electron Spectrosc. Relat. Phenom., 2010, **135**, 167-175.

15 D.C. Wei, Y.Q. Liu, Y. Wang, H.L. Zhang, L.P. Huang and G. Yu, Nano Lett., 2009, **9**, 1752-1758.
16 Z.S. Wu, A. Winter, L. Chen, Y. Sun, A. Turchanin, X.L. Feng and K. Müllen, Adv. Mater., 2012, **24**, 5130-5135.
17 H. Ming, J. Ming, X.W. Li, Q. Zhou, L.L. Jin, Y. Fu, J. Adkins, Z.H. Kang and J.W. Zheng, RSC Adv., 2013, **3**, 15613-15617.
18 Y. Qiao, X.L. Hu, Y. Liu, C.J. Chen, H.H. Xu, D.F. Hou, P. Hu and Y.H. Huang, J. Mater. Chem. A, 2013, **1**, 10375-10381.
19 C.Y. Ding, X.R. Qian, G. Yu and X.H. An, Cellulose, 2010, **17**, 1067-1077.
20 Y.C. Du, X.S. Zhu, X.S. Zhou, L.Y. Hu, Z.H. Dai and J.C. Bao, J. Mater. Chem. A 2015, **3**, 6787-6791.
21 Z.Y. Liang, Z.P. Lin, Y.M. Zhao, Y.Z. Dong, Q. Kuang, X.H. Lin, X.D. Liu and D.L. Yan, J. Power Sources, 2015, **274,** 345-354.
22 W.T. Kim, B.K. Min, H.C. Choi, Y.J. Lee and Y.U. Jeong, J. Electrochem. Soc., 2014, **161,** A1302-A1305.
23 W.T. Kim, Y.U. Jeong, Y.J. Lee, Y.J. Kim and J.H. Song, J. Power Sources, 2013, **244,** 557-560.
24 S.B. Ni, X.H. Lv, J.J. Ma, X.L. Yang and L.L. Zhang, Electrochim. Acta, 2014, **130,** 800-804.
25 X.S. Zhou, Y.X. Yin, L.J. Wan and Y.G. Guo, Adv. Energy Mater. 2012, **2**, 1086-1090.
26 Y.P. Wu, A.B. Fang and Y.Y. Jiang, J. Power Sources, 1998, **75** 201-206.